A Mixed-Ligand Iron-Sulfur Cluster ($C556S_{PsaB}$ or $C565S_{PsaB}$) in the F_X-Binding Site Leads to a Decreased Quantum Efficiency of Electron Transfer in Photosystem I

Ilya R. Vassiliev,* Yean-Sung Jung,* Lawrence B. Smart,‡ Rüdiger Schulz,‡ Lee McIntosh,‡ and John H. Golbeck*

*Department of Biochemistry and Center for Biological Chemistry, University of Nebraska, Lincoln, Nebraska 68588-0664; and ‡Department of Energy Plant Research Laboratory, Michigan State University, East Lansing, Michigan 48824-1312 USA

ABSTRACT The proposed structure of Photosystem I depicts two cysteines on the PsaA polypeptide and two cysteines on the PsaB polypeptide in a symmetrical environment, each providing ligands for the interpolypeptide F_X cluster. We studied the role of F_X in electron transfer by substituting serine for cysteine ($C565S_{PsaB}$ and $C556S_{PsaB}$), thereby introducing the first example of a genetically engineered, mixed-ligand [4Fe-4S] cluster into a protein. Optical kinetic spectroscopy shows that after a single-turnover flash at 298 K, the contribution of A_1^- (lifetime of 10 μs, 40% of total and lifetime of 100 μs, 20% of total) and F_X^- (lifetime of 500–800 μs, 10–15% of total) to the overall P_{700}^+ back reaction have increased in $C565S_{PsaB}$ and $C556S_{PsaB}$ at the expense of the back reaction from $[F_A/F_B]^-$. The electron paramagnetic resonance spectrum of F_X shows g-values of 2.04, 1.94, and 1.81 in both mutants and a similarly decreased amount of F_A and F_B reduced at 15 K after a single-turnover flash. These results indicate that the mixed-ligand (3 cysteines, 1 serine) F_X cluster is an inefficient electron carrier, but that a small leak through F_X still permits F_A and F_B to be reduced quantitatively when the samples are frozen during continuous illumination. The data confirm that F_X is a necessary intermediate in the electron transfer pathway from A_1 to F_A and F_B in Photosystem I.

INTRODUCTION

A unique and probably necessary component of Photosystem I (PS I) is F_X, a [4Fe-4S] cluster that is located on the reaction center heterodimer composed of the PsaA and PsaB polypeptides. F_X constitutes a rare example of an interpolypeptide iron-sulfur cluster, in which two of the cysteine ligands are provided each by member of the (hetero)dimer (Golbeck and Cornelius, 1986 Høj and Møller, 1986). PsaA and PsaB also bind the P_{700} chlorophyll a dimer, the primary electron donor, A_0, the primary chlorophyll acceptor, and A_1, the secondary phylloquinone acceptor (for review, see Golbeck and Bryant, 1991). As depicted in the 6-Å electron density map (Krauß et al., 1993), F_X occupies the same relative position in the PS I reaction center as does the non-heme iron in the purple bacterial reaction center and (presumably) in Photosystem II. However, unlike the non-heme iron, which is photochemically silent, F_X probably undergoes redox chemistry under physiologically relevant conditions. The midpoint potential of F_X/F_X^- couple is -705 mV (Chamorovsky and Cammack, 1982a), making it among the most electronegative iron-sulfur clusters known. This value is appropriate for its proposed function as an electron carrier between the intermediate phylloquinone acceptor A_1 ($E_m = -800$ mV) (Sétif and Bottin, 1989) and the terminal F_A and F_B clusters ($E_m = -530$ and -580 mV, respectively) (Evans and Heathcote, 1980).

Despite its prominent position in PS I, the role of F_X for forward electron transfer is not established fully. Reports on the kinetic properties of F_X (Crowder and Bearden, 1983; Sétif et al., 1984) have indicated that at low temperature there is little opportunity for an additional electron acceptor operating between A_1 and F_A/F_B. However, time-resolved electron paramagnetic resonance (EPR) spectroscopic studies at room temperature in PS I preparations that contain either the full complement of acceptors or only F_X (Moënne-Locoz et al., 1994; van der Est et al., 1994) support its participation in forward electron transfer. Optical spectroscopic studies on the kinetics of forward electron transfer from A_1^- in the presence and absence of F_A and F_B suggest that F_X is an obligatory component at room temperature (Lüneberg et al., 1994). More recent analysis of kinetics of electrogenic reactions in PS I provides added support for the participation F_X in serial electron transfer to F_B and F_A (Sigfridsson et al., 1995).

Unlike the purely kinetic approaches detailed above, we have introduced a genetic component in addressing the issue of F_X function in PS I. Our strategy has been to change the

Received for publication 21 March 1995 and in final form 23 July 1995.

Address reprint requests to Dr. John H. Golbeck, Department of Biochemistry, University of Nebraska-Lincoln, N138 Beadle Center, Lincoln, NE 68588-0664. Tel.: 402-472-2931; Fax: 402-472-7842; E-mail: jgolbeck@unlinfo.unl.edu.

Abbreviations used: A_1, the secondary electron acceptor in Photosystem I, a phylloquinone; Chl, chlorophyll; DCPIP, 2,6-dichlorophenol-indophenol; PS I, Photosystem I; DM-PS I, Photosystem I complex (containing F_X, F_A, and F_B iron-sulfur clusters) isolated using β-dodecyl maltoside; PS I core, Photosystem I core preparation (devoid of F_A and F_B iron-sulfur clusters) isolated from DM-PS I complex; P_{700}, the primary electron donor in Photosystem I, a chlorophyll a dimer; ΔA_{820}, photoinduced absorbance change at 820 nm; τ, lifetime of exponential decay component.

Published as Journal Series #11069 of the University of Nebraska Agricultural Research Division.

0006-3495/95/10/1544/10 $2.00

identity of the ligands to one of the cubane iron atoms in F_X with the expectation of altering electron transfer through the cluster. In an early screening, we found that PS I does not assemble upon substitution of $C565_{PsaB}$ for histidine or aspartate in *Synechocystis* sp. PCC 6803, most likely because of loss of one of the chemical bonds via the F_X cluster between the PsaB and PsaA polypeptides (Smart et al., 1993). However, we showed that substitution of serine for cysteine 565 on PsaB ($C565S_{PsaB}$) leads to the accumulation of PS I polypeptides and to the low temperature photoreduction of F_A and F_B. In a more detailed study (Warren et al., 1993b), we found that isolated PS I complexes from the $C565S_{PsaB}$ mutant contain either a [3Fe-4S] cluster or a mixed-ligand [4Fe-4S] cluster in the F_X site. The mixed-ligand [4Fe-4S] cluster had altered EPR spectroscopic properties (Warren et al., 1993b), including relatively narrow linewidths and altered *g*-values (2.015, 1.941, and 1.811) (the low-field *g*-value is uncertain). The [3Fe-4S] cluster was not present in freshly isolated thylakoid membranes, and it appeared only after detergent fractionation and purification. In contradiction to what appeared to be competent low-temperature electron transfer to F_A and F_B, the $C565S_{PsaB}$ mutant was incapable of photoautotrophic growth. The quantitative photoreduction of F_A and F_B at liquid helium temperatures, but the low steady-state spin concentration of F_X^- in continuous light, imply that this mutation leads to a decreased capacity of electron transport at room temperature. Because electron transfer studies based on EPR detection of iron-sulfur clusters are not possible at room temperature, we measured the efficiency of PS I electron transport using transient absorbance spectroscopy of P_{700}^+.

The region between cysteines 556 and 565 on PsaB (and the comparable region between cysteines 574 and 583 on PsaA) is thought to form a symmetrical PsaC-binding loops (Rodday and Biggins, 1993). We investigated, therefore, whether a substitution of a serine for cysteine 556 on PsaB ($C556S_{PsaB}$) would change the functional properties of PS I complex in a manner similar to $C565S_{PsaB}$. In this respect, it should be noted that in *Chlamydomonas reinhardtii* a substitution of a histidine for cysteine 560 on PsaB (which is equivalent to $C556H_{PsaB}$ in *Synechocystis* sp. PCC 6803) for histidine yielded a PS I-less mutant (Webber et al., 1993), as in the case of the $C565H_{PsaB}$ mutant reported by us previously (Smart et al., 1993).

The aim of this work is to determine whether electron throughput from P_{700} to F_A and F_B is affected in any given reaction center when F_X has been mutated to a mixed-ligand iron-sulfur cluster. We focus this study on the kinetics of electron transfer on the acceptor side of PS I in two F_X mutants, $C565S_{PsaB}$ and $C556_{PsaB}$. We find that the efficiency of forward electron flow through F_X is decreased considerably in both serine mutants, thus indicating that the cysteine ligands to F_X play a crucial role in facilitating a high efficiency of electron transfer from A_1 to F_A and F_B.

MATERIALS AND METHODS

A glucose-tolerant strain of *Synechocystis* sp. PCC 6803 was grown normally at 30°C in BG-11 medium supplemented with 5 mM glucose under light-activated heterotrophic growth (LAHG) conditions in the dark, as described previously (Anderson and McIntosh, 1991), with a 10-min pulse of white light every 24 h. Cultures were grown either in Erlenmeyer flasks filled with 50- to 1000-ml medium in a shaker or in 15-l carboys bubbled with air. Antibiotics were added, when appropriate, in the following concentrations: kanamycin, 5 $\mu g\ ml^{-1}$; spectinomycin, 20 $\mu g\ ml^{-1}$ (both from Sigma Chemical Co., St. Louis, MO).

Site-directed mutagenesis was performed with an oligonucleotide-directed in vitro mutagenesis kit as directed by the manufacturer (Amersham, Chicago, IL). DNA sequencing was done as described previously (Newman et al., 1994). Transformation of *Synechocystis* sp. PCC 6803 and segregation of homozygous mutants under LAHG-conditions was performed as described previously (Williams, 1988). Small-scale DNA preparations from the cyanobacteria were isolated from cells scraped from solid medium plates or harvested from small liquid cultures (Ohad and Hirschberg, 1992). The polymerase chain reaction was used to further confirm site-directed mutations with Amphi-Taq polymerase as directed by the supplier (Perkin-Elmer, Branchburg, NJ). A complete protocol for site-directed mutagenesis in the *psaB* gene leading to $C565S_{PsaB}$ was described previously (Smart et al., 1993). Selection and characterization protocols for the other mutant with substitution of a serine for cysteine at position 556 on PsaB ($C556S_{PsaB}$) were essentially the same.

After harvesting with a continuous flow rotor (DuPont Sorvall, Wilmington, DE), the cells were stored in BG-11 with 15% v/v glycerol at −95°C. Thylakoid membranes were isolated using the procedure described in Smart et al. (1991) with little modification. The cells were broken in buffer containing 20 mM MES (4-morpholineethanesulfonic acid), pH 7.2, 0.8 M sucrose, and protease inhibitors using a Bead Beater (Biospec Products, Bartelsville, OK). Membranes were precipitated with 40 mM $CaCl_2$, pelleted by centrifugation, and stored at −95°C until use.

Dodecyl maltoside Photosystem I complexes (DM-PS I) were prepared using a protocol based on methods described earlier (Chitnis and Chitnis, 1993; Warren et al., 1993b). Membranes were solubilized in 1% β-dodecyl maltoside (DM) (Calbiochem, La Jolla, CA) at 4°C for 1 h at Chl concentration of 1 $mg\ ml^{-1}$. DM-PS I complexes were isolated from the lower green band appearing after centrifugation of the solubilized membrane suspension in a sucrose density gradient (0.1–1.0 M for 24 h at 4°C) instead of the two-step column chromatography used in previous studies (Warren et al., 1993b). The isolated DM-PS I complexes were dialyzed in buffer containing 50 mM Tris, pH 8.3, resuspended with the same buffer containing 15% glycerol and 0.03% DM, frozen as small aliquots in liquid nitrogen, and stored at −95°C.

Photosystem I core preparations (PS I core) were isolated from wild-type DM-PS I complexes according to Golbeck et al. (1988). The DM-PS I complexes were suspended in 25 mM Tris buffer, pH 8.3, with 6.8 M urea and 100 mM NaCl to a Chl *a* concentration of 250 $\mu g\ ml^{-1}$ and incubated at room temperature to allow dissociation of PsaC, PsaD, and PsaE polypeptides. The progress of the reaction was monitored by measuring the ΔA_{820} kinetics (see below) every 10 min. The procedure was stopped by 6× dilution of the reaction media with 25 mM Tris-HCl buffer, pH 8.3, and 100 mM NaCl when the tens-of-millisecond decay phase was eliminated almost completely (~50–80 min). The sample was purified and concentrated by forcing the suspension through Amicon YM-100 membrane with nitrogen gas at 60 psi. The PS I cores were resuspended in 25 mM Tris buffer, pH 8.3, with 15% glycerol and 0.03% DM, frozen as small aliquots in liquid nitrogen, and stored at −95°C.

Samples for optical experiments were suspended in 25 mM Tris buffer, pH 8.3, with 4 mM 2,6-dichlorophenol-indophenol (DCPIP) and 10 mM sodium ascorbate (unless otherwise indicated) to a Chl *a* concentration of 50 $\mu g\ ml^{-1}$ in a Thumberg tube. Air was evacuated subsequently with a vacuum pump and substituted with high purity nitrogen gas. The samples were transferred to a 10 mm × 2 mm quartz cuvette with a stopper for optical analysis. This procedure, as well as preparation of all chemical solutions, was performed in an anaerobic chamber (Coy Products, Grass

Lake, MI). For normalizing of all optical data, the Chl *a* was extracted and measured in the samples after completing the optical measurements.

Transient absorbance changes of P_{700} at 820 nm (ΔA_{820}) were measured from the microseconds to tens-of-seconds time domain with a laboratory-built double-beam spectrometer. The measuring beam at 820 nm was provided by a DC 25 F semiconductor diode laser (Spindler and Hoyer, Göttingen, Germany) with an output power of 50 mW. For correction of the laser instability, the beam was split; the measuring beam was passed through the quartz cuvette containing the sample (pathlength, 1 cm), whereas the reference beam was passed through an attenuating variable density filter. The beams were directed to a pair of reverse-biased planar-diffused silicon photodiode detectors (United Detector Technology, Model PIN-10D) shielded by RG-10 cutoff filters. The photocurrents were converted to voltages with 1-kΩ resistors, and the difference between the signal and reference was measured in real time at 8-bit vertical resolution with a Tektronix 11A33 DC-coupled differential comparator (150-MHz bandwidth) plugged into a Tektronix DSA 601 digital signal analyzer (Tektronix, Beaverton, OR). The excitation beam was provided by a frequency-doubled, Q-switched Nd-YAG laser (DCR-11, Spectra-Physics) operating at 532 nm. The pulse width at half-maximum was 10 ns, and the flash energy was 135 mJ. Data were acquired at four different time scales (2048 points each) using zoom window capacities of the DSA 601. The sweep was triggered by a fast photodiode (875 PIN detector, Newport Corp., Irvine, CA) that monitored stray light of the Nd-YAG laser pulse via a Tektronix 11A52 amplifier (600-MHz bandwidth) plugged into the DSA 601. The set of data for each sample was acquired as four kinetic traces in the DSA 601 memory and transferred to a Macintosh Quadra computer via a National Instruments NB-GPIB/TNT board and stored as separate files. The nonoverlapping parts of kinetics corresponding to different time domains were linked to yield an overall decay curve using Igor Pro 2.02 (WaveMetrics, Lake Oswego, OR). This procedure also reduced total number of points to 4608 by interpolating the set of points starting from the 513th point to a log-distributed time scale vector. The curves were fitted to "sum of several exponentials with baseline" using the Marquardt algorithm in Igor Pro. The user-defined fit function enabled a fit up to seven exponentials with all amplitudes and rate constants set free during the fit. The results of the fit were output automatically as the overall fit curve, individual components curves, residuals, and a table of values of lifetimes and percentages of components' amplitudes and their SE of fit. In most cases, the fit comprised a baseline component accounting for long-term phases and/or possible drift of signal zero during long time scale acquisition. The quality of the fit was estimated using standard techniques including analyses of the residuals plots and comparison of the χ^2 values and SE of the fit parameters between different fits. Using this approach to deconvoluting the kinetics, the PS I back reactions can be compared visually on a log time scale, and the ratio between the different pathways that contribute to the back reactions with P_{700}^+ can be estimated. Depending on the number of acceptors and on their relative contribution to the overall back reaction, the kinetics can be fit accurately by a sum of four to six exponentials. Fitting of all components, including those that are of yet uncertain nature, or resulting from reactions with mediators, gives a precise determination of components of biological significance.

EPR studies were performed using a Bruker ECS-106 X-band spectrometer equipped with either a standard-mode (ER/4102 ST) or dual-mode resonator (DM/4116). Cryogenic temperatures were maintained with an Oxford liquid helium cryostat and an ITC4 temperature controller. Microwave frequency was measured with a Hewlett-Packard 5340A frequency counter and recorded in memory. Sample temperatures were monitored by a calibrated thermocouple situated beneath the 3-mm inner diameter quartz sample tube and referenced to liquid nitrogen. Continuous actinic illumination of the sample was provided by a 150-W Model 66057 xenon arc source (Oriel Corp., Stratford, CT) filtered through 5 cm of water and passed through a heat-absorbing filter to remove the near infrared wavelengths. Samples used for EPR measurements upon steady-state illumination contained either 0.5 mg ml^{-1} (wild-type) or 1 mg ml^{-1} (mutants) Chl, 1 mM sodium ascorbate, 30 μM DCPIP in 50 mM Tris-HCl, pH 8.3. For single-flash excitation, the samples were suspended at a chlorophyll concentration of 200 μg ml^{-1} in the same buffer containing 60% glycerol, and the Nd-YAG laser (see above) beam was diverted directly into the EPR cavity. For chemical reduction of the F_A and F_B clusters, samples were suspended at a chlorophyll concentration of either 0.5 mg ml^{-1} (wild-type) or 1 mg ml^{-1} (mutants) in 250 mM glycine, pH 10, with 50 mM sodium dithionite. Spin quantitations were made at a power level at least one order of magnitude below the half-saturation parameter, $P_{1/2}$. Simulations of the EPR spectra were performed using the "Xpow" version of "Qpow" (Belford and Nilges, 1979) after recompiling the source code in MacFortran (Absoft Corp., Rochester Hills, MI) to run on a Macintosh 7100/80 RISC-based computer. All further data manipulations and graphics were performed using IGOR Pro (WaveMetrics).

RESULTS

Kinetic analysis of electron acceptors in wild-type PS I

To study the functioning of PS I in the F_X mutants at physiological temperatures, we measured flash-induced absorbance changes of P_{700}^+ at 820 nm. The time constants derived from the kinetic transients were used to identify the relative contributions of various electron acceptors to P_{700}^+. The lifetimes of back electron transfer from different components of the PS I acceptor side to P_{700}^+ range from tens of nanoseconds (A_0); tens of microseconds (A_1); hundreds of microseconds (F_X); and tens of milliseconds (F_A/F_B) (for review, see Golbeck, 1987). We first carried out a verification protocol on wild-type PS I complexes to determine whether the computer-fitted exponentials correlated with known back reactions of P_{700}^+. In a number of previous studies, the kinetics of the 820-nm absorbance change has been investigated in a relatively narrow time window appropriate for fitting to a limited number of components at a time (usually 1–3 exponentials and a baseline accounting for slower components). Using the described setup (see Materials and Methods), we monitored a continuum of kinetic phases corresponding to P_{700}^+ back reactions with all endogenous acceptors from A_1 to F_A/F_B, as well as those arising from reactions of P_{700}^+ with redox agents in the media.

Fig. 1 *A* shows ΔA_{820} decay kinetics measured in DM-PS I complexes isolated from wild-type cells of *Synechocystis* sp. PCC 6803. The fastest component resolved in the complex has a lifetime of 11 μs, which can be attributed to the relaxation of a P_{700}^+ triplet (Sétif and Brettel, 1990) and/or to a back reaction from A_1^- (Warren et al., 1993a). Its contribution to the overall decay is only ~4%, and the precision of the fit parameters is rather low, because it is fitted on a background of slower components and near the limit of the time resolution. The next component resolved in the complex has a lifetime of 611 μs, and its contribution to overall signal is as low as 2%. This lifetime corresponds to back-transfer of electrons from F_X^- (Sétif and Bottin, 1989; Parret et al., 1989). The next two components, with lifetimes of 12.3 and 97.3 ms, should be ascribed to a back reaction from F_A^- and/or F_B^- (these acceptors cannot be distinguished from one another at room temperature). It is very likely that the component with a half-time of 30 ms reported in a number of earlier studies (Sauer et al., 1978; Golbeck et al., 1988)

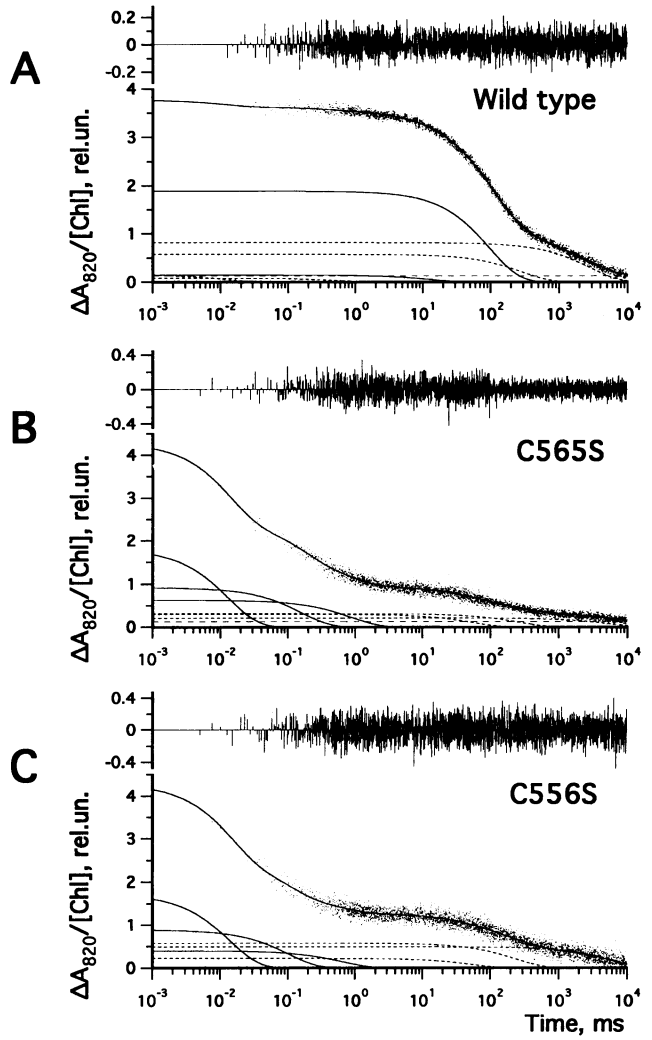

FIGURE 1 Kinetics of absorbance change at 820 nm measured at room temperature in DM-PS I preparations from the wild-type (*A*), $C565S_{PsaB}$ (*B*), and $C556S_{PsaB}$ (*C*) *Synechocystis* sp. PCC 6803. The reaction media is 25 mM Tris buffer, pH 8.3, with 0.03% DM, 10 mM sodium ascorbate, and 4 μM DCPIP; the chlorophyll concentration is 50 μg ml^{-1}. Each trace (*dots*) is an average of 16 measurements taken at 50-s intervals. The multiexponential fit is overlaid as a solid line; residuals of the fit shown at the top of the graph. The major individual exponential components are shown as solid lines. The parameters of the exponential fit are summarized in Table 1.

TABLE 1 Parameters of the multiexponential fit of ΔA_{820} kinetics of PS I samples in 25 mM Tris buffer, pH 8.3, with 0.03% DM, 10 mM sodium ascorbate, and 4 μM DCPIP (Fig. 1). τ, components' life times; *A*, components' contribution (%) to the total signal amplitude

A. Wild-type DM-PS I

τ	$\pm\tau$	A (%)	$\pm A$ (%)
11 μs	17 μs	4.0	9.0
611 μs	156 μs	2.1	0.3
12.3 ms	2.7 ms	3.8	0.6
97.3 ms	6.1 ms	50.0	4.1
282.6 ms	57.9 ms	15.2	4.2
2.8 s	0.1 s	21.5	0.5
Baseline		3.4	0.2

B. Wild-type PS I core

τ	$\pm\tau$	A (%)	$\pm A$ (%)
7 μs	1 μs	14.7	1.3
58 μs	7 μs	7.8	0.5
389 μs	12 μs	22.9	0.4
1.74 ms	0.04 ms	36.3	0.4
7.9 ms	0.3 ms	8.8	0.4
128.8 ms	2.6 ms	4.3	0.1
Baseline		5.2	0.01

C. C565S DM-PS I

τ	$\pm\tau$	A (%)	$\pm A$ (%)
13 μs	1 μs	42.1	2.6
156 μs	15 μs	21.3	1.0
853 μs	56 μs	14.5	1.0
51.9 ms	6.6 ms	6.9	0.9
258.1 ms	41.0 ms	7.2	0.8
5.4 s	1.7 s	4.9	0.5
Baseline		3.0	0.7

D. C556S DM-PS I

τ	$\pm\tau$	A (%)	$\pm A$ (%)
14 μs	3 μs	40.5	4.1
100 μs	21 μs	20.7	2.7
637 μs	94 μs	9.2	1.5
53.4 ms	15.0 ms	5.2	1.7
234.4 ms	32.4 ms	13.4	1.5
6.1 s	1.4 s	11.4	1.0
Baseline		−0.3	1.3

was actually a mixture of the above two components. To verify this assumption, we ran a two-exponential fit of the wild-type data from Fig. 1 *A* in the same time domain as in earlier work (Golbeck et al., 1988). This decomposition yielded a 38.1% contribution from a 43.9 ms component (which is equal to half-time of 30 ms), a 2.3% contribution from a 650 μs component, and a 59.6% baseline, but the quality of the fit was lower than in the case of the multiexponential fit shown in Fig. 1 *A* and Table 1 *A*. Also, the 97.3-ms lifetime of the major component found in our preparations is very close to the 90-ms lifetime ascribed to charge recombination between F_A^- and P_{700}^+ based on relaxation kinetics of flash-induced electrogenic changes in PS I (Sigfridsson et al., 1995).

The slowest components with lifetimes of 282.6 ms and 2.8 s are probably a result of P_{700}^+ reduction from exogenous chemical(s) undergoing redox reactions. In the wild-type PS I complex, the contribution of the component with a lifetime around 280 ms was increased when the DCPIP concentration was increased from 2 to 80 μM, whereas the slowest one with a lifetime of 3–4 s was suppressed completely (not shown). The amplitude and kinetics of the ΔA_{820} signal did not change from flash to flash if the dark interval was

>30–40 s, indicating that this time is sufficient for the complete reduction of P_{700}^+. We suspect that the slow kinetic phases arise in reaction centers where endogenous electron acceptor(s) have oxidized F_A^- and/or F_B^-, thereby allowing exogenous redox donors to reduce P_{700}^+ in relatively slow time periods.

Attempts to increase the number of components in the fit of the wild-type PS I complex did not improve its quality, yielding instead components with about the same lifetimes but with relatively high errors. The magnitude and lifetimes of the components varied somewhat from preparation to preparation, but the general trend in the hierarchy of the lifetimes remained identical.

The identity of the resolved kinetic components can be illustrated further by comparing the ΔA_{820} kinetics of a PS I complex with that of an isolated PS I core. It was shown earlier that when the PsaC protein is removed with 6.8 M urea the ~30-ms ΔA_{820} transient due to the $[F_A/F_B]^-$ back reaction is replaced with a 1-ms component arising from the F_X^- back reaction (Parrett et al., 1989). As compiled in Table 1 *B*, the contribution of decay components in the PS I core in the tens of milliseconds time domain (and slower phases approximated with a baseline) is <20%; a majority of the kinetics (~60%) occur with lifetimes of 389 μs and 1.74 ms, which are attributed to the biphasic back reaction from F_X^-. It is likely that these two components were not distinguished in a previous study (Parrett et al., 1989), thus yielding a single component with a half-time of ~1 ms (lifetime of 1.4 ms). A PS I deletion mutant of *Synechocystis* sp. PCC 6803 that lacks PsaC (as well as PsaD and PsaE) shows a similar biexponential back reaction between P_{700}^+ and F_X^- with lifetimes of 438 and 1.56 μs (Yu et al., 1995). Hence, the existence of two kinetic phases of the F_X^- back reaction does not appear to be an artifact of the urea treatment but, rather, exists as an inherent property of this acceptor.

The remaining back reactions in the PS I core occur with lifetimes of 7 and 58 μs. These two components are most likely to arise from the A_1^- back reaction, which was reported to have decay half-times ranging from 10 to 250 μs (Sétif et al., 1984; Brettel et., 1986; Brettel, 1989; Sétif and Bottin, 1989). These values, however, should be treated with caution, because they were determined in the presence of reduced F_A^- and F_B^- (and in some instances F_X^-). Very recent studies of flash-induced A_1 absorbance difference spectra in the near-UV of a P_{700}-A_1 core devoid of F_X, F_A, and F_B indicate that the A_1^- back reaction is inherently biphasic, with half-times of 10 and 110 μs and present at a ratio of ~2:1 (Warren et al., 1993a; Brettel and Golbeck, 1995). Although the origin of two-exponential kinetics of back reaction between A_1^- and P_{700}^+ is not clear, it should be noted that similar two-exponential kinetics attributed to existence of two reaction center conformers was found for back reactions of primary and secondary quinones (Q_A and Q_B) in reaction centers of *Rhodopseudomonas viridis* (Gao et al., 1991).

Kinetic analysis of electron acceptors in the $C565S_{PsaB}$ mutant

Fig. 1 *B* shows the ΔA_{820} decay kinetics and the multiexponential fits of the data measured in PS I complexes from the $C565S_{PsaB}$ mutant (Fig. 1 *C* will be discussed later). The overall amplitude of ΔA_{820} relative to chlorophyll content is similar to that of the wild-type, which indicates the same amount of photoactive P_{700} in the two PS I complexes. The results of the fit show that the kinetics of the $C565S_{PsaB}$ is considerably different from the kinetics of the wild-type (compare Fig. 1, *A* and *B*). In the wild-type, >53% of P_{700}^+ is reduced via a back reaction from F_A^- and/or F_B^- (Table 1 *A*), whereas in the $C565S_{PsaB}$ mutant this back reaction, which is resolved as a single 51.9-ms component (Table 1 *C*) contributes no more than 7% to P_{700}^+. As seen from the results of the decomposition, >63% of the back reaction in the $C565S_{PsaB}$ mutant is derived from A_1^- (13- and 156-μs components), and ~15% by a back reaction from F_X^- (853-μs component). One should note in Table 1 *B* that in the wild-type PS I core that the contribution of the A_1^- back reaction is ~3 times lower than that of the F_X^- back reaction. This may arise from a minority of reaction centers in which F_X has been damaged by the treatment to remove PsaC, or it may reflect an equilibrium between A_1 and F_X that becomes apparent in the absence of F_A and F_B. The PsaC-deletion mutant of *Synechocystis* sp. PCC 6803 shows nearly identical kinetics to that of the urea-isolated PS I core preparations (Yu et al., 1995), thereby lending support to the latter interpretation. The F_X mutant complex, therefore, differs not only from wild-type PS I complex, but also from the wild-type PS I core, thus highlighting the fact that this mutation does not block electron transfer from F_X to F_A/F_B but, rather, functions as an inefficient electron acceptor from A_1^-. In previous work with the $C565S_{PsaB}$ mutant (Warren et al., 1993b), the total measurement scale of 100 μs did not allow us to resolve ΔA_{820} phases except for the 10-μs phase attributed to the A_1^- back reaction. This phase accounted for 25% of the signal amplitude and was not seen in the wild-type PS I complex. However, the half-time of this phase and its relative contribution is in good agreement with present data, which on a log time scale give a much better indication of the electron transfer kinetics to P_{700}^+.

Another approach to studying electron transfer before F_A and F_B is to reduce chemically the clusters in the dark before illumination. Under these conditions, a ΔA_{820} transient after a single-turnover flash reflects the back reactions of F_X^- (as well as preceding electron acceptors). As a precaution against irreversible double-reduction of A_1 (Sétif and Bottin, 1989), only one excitation flash was used in these experiments. Fig. 2 shows results of such an experiment with the wild-type PS I complex and the $C565S_{PsaB}$ PS I complex after F_A and F_B were reduced with sodium dithionite at pH 10 (confirmed by EPR spectroscopy; see Fig. 4). A comparison of the kinetic decomposition data (Table 2, *A* and *B*) shows that although >67% of the back reaction occurs from F_X^- in the wild-type, the contribution of

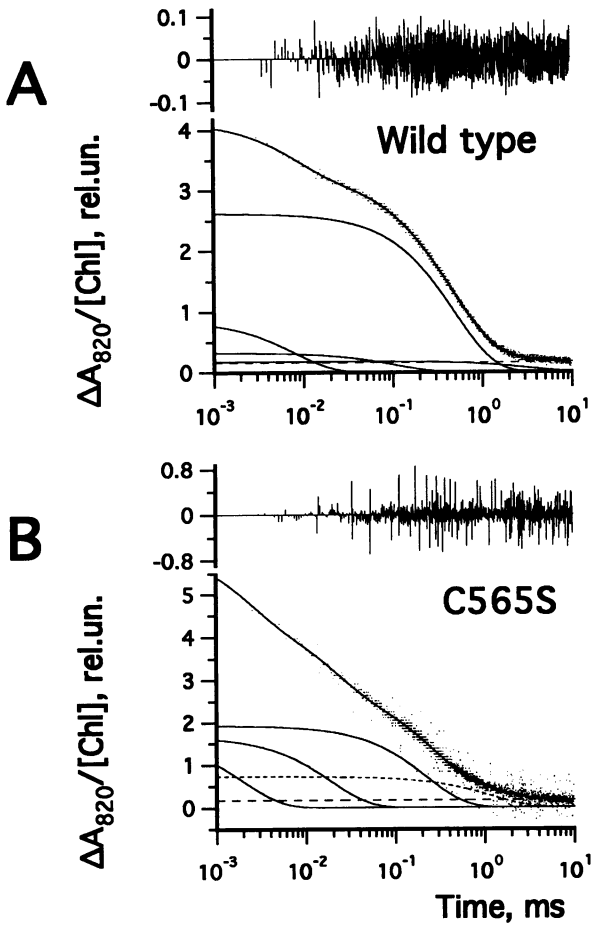

FIGURE 2 Kinetics of absorbance change at 820 nm measured at room temperature in preparations from wild-type (*A*) and $C565S_{PsaB}$ (*B*) *Synechocystis* sp. PCC 6803 with the F_A and F_B clusters prereduced with 50 mM dithionite in 100 mM glycine buffer, pH 10, with 0.03% DM. The chlorophyll concentration is 50 $\mu g\ ml^{-1}$. The samples were illuminated by a single saturating laser flash. Fit parameters are summarized in Table 2.

this acceptor to the back reaction is <12% in the $C565S_{PsaB}$ mutant. Instead, >60% of the back reaction (the 19- and 222-μs kinetic phases) in the $C565S_{PsaB}$ mutant occurs from A_1^-. There is also indication of a faster component ($\tau \approx 2$ μs), but the errors are relatively high because it appears on the border of the time resolution, with a rather low signal-to-noise ratio due to the single acquisition. Exclusion of this component leads to even higher contribution of the A_1^- back reaction to the overall kinetics.

Kinetic analysis of electron acceptors in the $C556S_{PsaB}$ mutant

The F_X cluster is bound by cysteines 574 and 583 on PsaA and by cysteines 556 and 565 on PsaB. Biggins and coworkers (Rodday et al., 1993) have modeled this region and suggested that the intervening sequences between the homologous cysteines form two flexible loops that participate in the binding of PsaC. The proposed structure thus depicts the two cysteines on each protein in a relatively symmetrical

TABLE 2 Parameters of the multiexponential fit of ΔA_{820} kinetics of PS I samples in 100 mM glycine buffer, pH 10, with 0.03% DM, and 50 mM sodium dithionite

A. Wild-type DM-PS I

τ	$\pm\tau$	A (%)	$\pm A$ (%)
8 μs	1 μs	21.0	0.8
102 μs	10 μs	7.8	0.5
502 μs	8 μs	63.2	0.4
3.2 ms	0.6 ms	4.3	0.4
Baseline		3.8	0.2

B. C565S DM-PS I

τ	$\pm\tau$	A (%)	$\pm A$ (%)
2 μs	1 μs	26.9	26.3
19 μs	2 μs	27.2	2.0
222 μs	10 μs	31.3	0.8
1.2 ms	0.1 ms	11.8	0.9
Baseline		2.8	0.1

configuration connecting two α-helices near the surface of the membrane. We studied, therefore, electron transfer efficiencies and kinetics in a mutant where cysteine 556 was changed to serine (Fig. 1 *C*). As shown in Table 1 *D*, the lifetimes of the P_{700}^+ A_1^- back reaction in the $C556S_{PsaB}$ mutant are biphasic with lifetimes of 14 and 100 μs, the two phases occur at the expected ratio of ~2:1 and, together, these kinetics account for >60% of the back reaction. The back reaction from F_X (lifetime of 637 μs) and from F_A/F_B (lifetime of 53.4 ms) constitute only 9 and 5% of the overall kinetics, respectively, and ~25% of the kinetics appear to be due to forward donation from exogenous donors to P_{700}^+. A sample that was treated with sodium dithionite at pH 10 to reduce F_A and F_B had kinetics nearly identical to that of $C565S_{PsaB}$ (not shown). The room temperature optical properties of the electron acceptor system in the $C556S_{PsaB}$ mutant complex, therefore, are similar to the $C565S_{PsaB}$ mutant.

EPR spectroscopic properties of the $C556S_{PsaB}$ and $C565S_{PsaB}$ mutants

To assess further the properties of the F_X cluster, we measured the low-temperature EPR spectra of wild-type, $C565S_{PsaB}$, and $C556S_{PsaB}$ PS I complexes. Under mildly oxidizing conditions, we could not find any $[3Fe\text{-}4S]^{1+}$ clusters in the $C556S_{PsaB}$ PS I complex, whereas in the $C565S_{PsaB}$ PS I complex, the $[3Fe\text{-}4S]^{1+}$ cluster was detected in very small amounts (<5%), and certainly much less than the amount quantitated on the basis of the relative number of spins under the same measurement conditions as in the previous paper (Warren et al., 1993b). A search for $[3Fe\text{-}4S]^0$ clusters in the $C556S_{PsaB}$ PS I complex around $g = 10$ using parallel-mode EPR spectroscopy was also negative (a reduced [3Fe-4S] cluster is a paramagnetic S = 2 system). In the present study, we were able to yield a

much more homogenous preparation from both mutants by using a milder conditions of the complex isolation (see Materials and Methods). Our data thus support our earlier suggestion that the population of [3Fe-4S] clusters in the $C565S_{PsaB}$ PS I mutant results from loss of iron from F_X during detergent fractionation.

As shown in Fig. 3, illumination of ascorbate-reduced, dark-frozen samples leads to irreversible photoreduction of F_A at g = 2.047, 1.944, and 1.852 and F_B at g = 2.069, 1.930, and 1.881. The g-values and the ~5:1 ratio of F_A to F_B (calculated from computer simulations and double integration of the scaled spectra), are similar in the $C556S_{PsaB}$ and $C565S_{PsaB}$ mutant PS I complexes as well as in the wild-type PS I complex. When the mutant samples are frozen during illumination, resonances are observed at g = 2.047, 1.940, 1.921, and 1.885 characteristic of magnetic interaction between reduced F_A^- and F_B^-. This indicates that the degree of coupling between F_A and F_B is not affected by the cysteine-to-serine substitutions on the PsaB polypeptide. Fig. 4 shows the difference between the photoaccumulated and "dark-frozen" EPR spectra after prereduction of F_A and

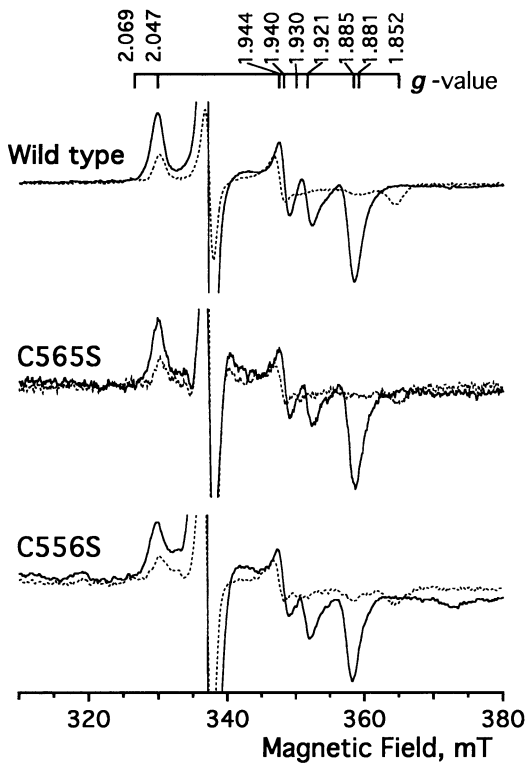

FIGURE 3 EPR spectra of the Wild-type, $C565S_{PsaB}$, and $C556S_{PsaB}$ PS I in the presence of 1 mM sodium ascorbate and 30 μM DCPIP in 50 mM Tris-HCl, pH 8.3. The chlorophyll concentration was 1 mg ml^{-1} for the wild-type and 0.5 mg ml^{-1} for the $C565S_{PsaB}$ and $C556S_{PsaB}$ mutants. The mutant traces were expanded in software by a factor of two to normalize all three traces to an equivalent P_{700} concentration. (- - - -) Spectrum after freezing the sample in darkness and illumination at 15 K. (——) Spectrum after freezing the sample during illumination. Spectrometer conditions: temperature, 15 K; microwave power, 20 mW; microwave frequency, 9.453 GHz; receiver gain, 2×10^4; modulation amplitude, 1 mT at 100 kHz; magnetic field, 340 mT with scan width of 100 mT.

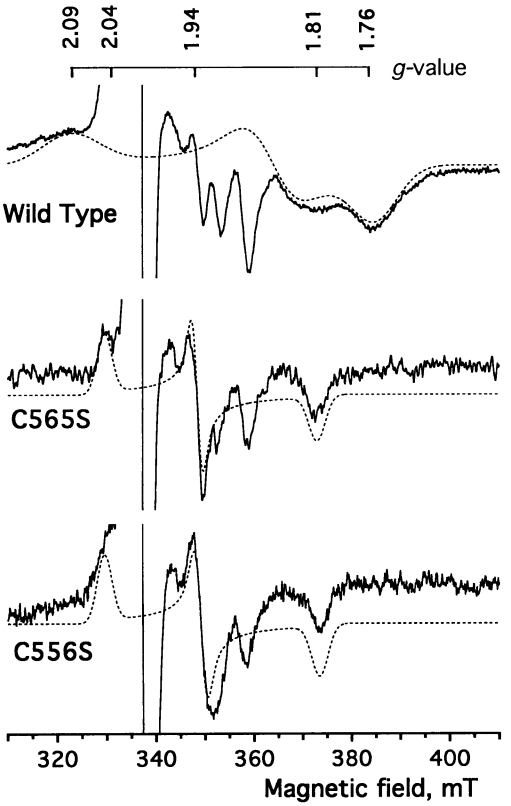

FIGURE 4 EPR spectra of the wild-type, $C565S_{PsaB}$, and $C556S_{PsaB}$ PS I with F_A and F_B clusters prereduced with dithionite at pH 10 and illuminated during freezing to 9 K (wild-type) or 12 K (mutants). (——) Experimental spectrum. The background spectra was measured in a dark-adapted sample frozen to 9 K (wild-type) or 12 K (mutants) and subtracted from the light-induced spectra. The chlorophyll concentration was 1 mg ml^{-1} for the wild-type and 0.5 mg ml^{-1} for the $C565S_{PsaB}$ and $C556S_{PsaB}$ mutants. The mutant traces were expanded in software by a factor of two to normalize all three traces to an equivalent P700 concentration. (- - - -) Simulated spectrum. The parameters for the simulations were: wild-type, g = 2.0916, 1.8550, and 1.7540 and linewidths of 200, 150, and 135 MHz, respectively; $C565S_{PsaB}$, g = 1.0488, 1.9335, and 1.8071 and linewidths of 50, 35, and 50 MHz; $C556S_{PsaB}$, g = 2.0488, 1.9380, and 1.8100 and linewidths of 50, 30, and 50 MHz. Spectrometer conditions: temperature, 12 K; microwave power, 40 mW; microwave frequency, 9.449 GHz; receiver gain, 2×10^4; modulation amplitude, 3.2 mT at 100 kHz; magnetic field, 360 mT with scan width of 100 mT.

F_B with sodium dithionite at pH 10. Both the $C565S_{PsaB}$ and $C565S_{PsaB}$ PS I complexes exhibit a rhombic set of resonances with nearly identical g-values of 2.04, 1.94, and 1.81 and with relatively narrow linewidths compared with the wild-type PS I complex (the resonances between 345 and 360 mT represent subtraction artifacts due to incomplete reduction of F_A and F_B with dithionite). Because of the similarity of the spectra, the clusters represented by the $C565S_{PsaB}$ and $C565S_{PsaB}$ mutant PS I complexes are both termed F_X'. When both mutant complexes are frozen in darkness with F_A and F_B prereduced, a component with a highfield resonance at g = 1.81 appears on illumination at 12 K, and the midfield resonance at g = 1.94 becomes more intense. The g = 1.81 resonance disappears in both mutant

complexes after turning off the light (data not shown; for the $C565S_{PsaB}$ mutant results, see Warren et al., 1993b). As in the $C565S_{PsaB}$ complex (Warren et al., 1993b), the resonances in the $C556S_{PsaB}$ complex are observed only over a narrow temperature range, attaining a maximum at 12–14 K (data not shown). The spin concentration of the F_X' cluster in $C565S_{PsaB}$ is ~25% expected from the amount of F_A and F_B (determined from double integration of computer simulations, depicted as the dotted lines in Fig. 4). This is most likely a reflection of a relatively low quantum yield of F_X reduction revealed earlier in the room temperature optical experiments. Because the $P_{700}^+ F_X^-$ back reaction is reversible at cryogenic temperatures, the amount of steady-state F_X^- in the light will be a function of the rates of forward reaction from A_1^- and the back reaction rates from A_1^- and F_X^-. Given that the latter remain unchanged, the lower the efficiency of electron transfer from A_1^-, the lower will be the spin concentration of F_X'. The similarity in the optical kinetic properties of the modified F_X' cluster in both the $C556S_{PsaB}$ and the $C565S_{PsaB}$ mutants thus extends to the g-values and linewidths of the resonances (Fig. 4), and to the spin relaxation properties as inferred from the temperature dependence and $P_{1/2}$ value (data not shown). This is probably not coincidental and may reflect the stereochemical symmetry of the two cysteine ligands in terms of F_X binding.

Low temperature quantum efficiencies of the $C565S_{PsaB}$ and $C556S_{PsaB}$ mutants

To verify that the photoreduction of F_A and F_B also occurs with a lower quantum efficiency at cryogenic temperatures, we determined the amount of F_A photoreduction using EPR spectroscopy after a single-turnover flash. It is known that the photoreduction of the F_A cluster is irreversible at temperatures <25 K and that it occurs with a higher yield than the photoreduction of F_B (Chamorovsky and Cammack, 1982b). We measured, therefore, the g = 1.944 midfield resonance of F_A^- under experimental conditions similar to those of Fig. 3 (*dashed lines*) except that illumination of a dark-frozen sample at 15 K was provided with a train of single-turnover saturating flashes from a Nd-YAG laser at 5-min intervals. As shown in Fig. 5, the intensity of the midfield resonance from F_A^- in the $C565S_{PsaB}$ mutant lies well below that of the wild-type when the experimental sets of data are normalized after a very large number of flashes (~50) to simulate the effect of continuous illumination. Similar results were obtained with the $C556S_{PsaB}$ mutant (data not shown). The higher number of quanta required for stabilization of the electron on F_A in the $C565S_{PsaB}$ and $C556S_{PsaB}$ mutants at low temperature, as well as the low yield of the back reaction from $[F_A/F_B]^-$ shown in the room temperature ΔA_{820} kinetics, show that the photoreduction of F_A occurs with a decreased quantum efficiency at temperatures down to 15 K.

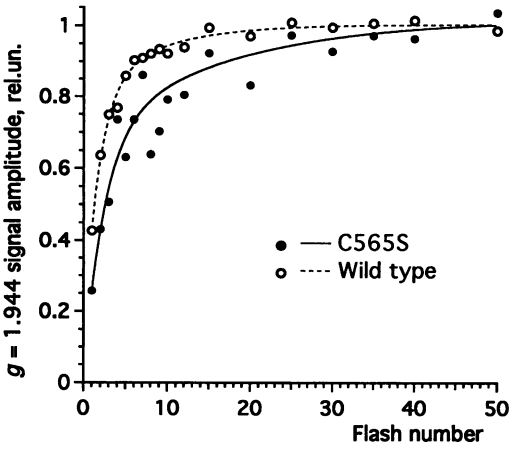

FIGURE 5 Flash saturation dependency of amplitude of g = 1.944 resonance (see Fig. 2) of wild-type and $C565S_{PsaB}$. The samples were frozen to 15 K in darkness and illuminated in the EPR cavity with train of 10-ns flashes from a Nd-YAG laser. Samples were suspended in 25 mM Tris buffer, pH 8.3, with 1 mM sodium ascorbate and 30 μM DCPIP and 60% (v/v) glycerol; the chlorophyll concentration was 200 $\mu g\ ml^{-1}$. The data are normalized to the average value of the last two flashes points.

DISCUSSION

To our knowledge, the $C565S_{PsaB}$ and $C556S_{PsaB}$ mutants represent the first examples of a genetically engineered [4Fe-4S] cluster supported by three cysteines and one serine. The properties of this mixed-ligand F_X cluster are inherently of interest because it is only one of two known examples of a interpolypeptide [4Fe-4S] cluster with cysteine ligands contributed by two polypeptides. Previous studies of cysteine-to-serine mutations in iron-sulfur clusters have focused primarily on soluble [2Fe-2S] ferredoxins. Site-directed changes in three of the four cysteines in a [2Fe-2S] ferredoxin from *Clostridium pasteurianum* show that serines can support formation of an intact iron-sulfur cluster (Fujinaga et al., 1993). Results in *Anabaena* 7120 vegetative ferredoxin have shown that serine can replace cysteine in each of the four positions and still support assembly of a (relatively) stable cluster (Cheng et al., 1994; Holden et al., 1994). It is generally assumed that the serine oxygen provides a ligand to the [2Fe-2S] cluster in the ferredoxin site-directed mutants. This assessment is supported by studies of [2Fe-2S] model compounds in which sulfur-terminal ligands are replaced by oxygen (Beardwood and Gibson, 1985; Salifoglou et al., 1988). The question of whether the serine oxygen provides a ligand to the cubane iron in F_X or whether it simply provides a suitable environment for water or OH^- or β-mercaptoethanol to function as an exogenous ligand remains open at this time. In the present work, we show that such a mixed-ligand cluster can be functional enough to mediate electron transfer, albeit with lower efficiency, to the terminal iron-sulfur clusters.

A primary motivation of this work was to probe the origin of the apparent disparity between the quantitative photoreduction of F_A and F_B and the low steady-state spin concen-

tration of the mixed-ligand F_X' cluster in the $C565S_{PsaB}$ (Smart et al., 1993) and $C556S_{PsaB}$ mutants (this paper). Using room temperature optical kinetic spectroscopy and low temperature EPR spectroscopy after a single-turnover flash, we show that the substitution of serine for cysteines in positions 556 and 565 of PsaB results in inefficient electron transfer on the acceptor side of PS I. The presence of a prominent back reaction from A_1^- (lifetimes of ~10 and 100 μs) indicates that a majority of the electrons do not pass from A_1^- to F_X in the $C565S_{PsaB}$ and $C556S_{PsaB}$ complexes (Fig. 1, Table 1). Given that the absolute amplitude of the P_{700} absorbance change is about the same on a chlorophyll basis in the $C556S_{PsaB}$ and the $C565S_{PsaB}$ mutants and in wild-type PS I, the increase in contributions of the A_1^- (and F_X^-) back reactions to P_{700}^+ reduction must occur at the expense of the $[F_A/F_B]^-$ back reaction (Fig. 1, Table 1); hence, only a minority of the electrons reach the F_A/F_B terminal iron-sulfur clusters on a single excitation.

The quantitative photoreduction of F_A and F_B comes about because charge separation with P_{700} is irreversible at cryogenic temperatures: the large number of turnovers in each center produced by continuous illumination of the sample in the EPR cavity over a period of time results in complete charge separation of the $P_{700}^+ [F_A/F_B]^-$ state. Accordingly, the lower the quantum efficiency, the fewer the number of $P_{700}^+ [F_A/F_B]^-$ centers generated on each single-turnover flash and the greater number of flashes is required to achieve quantitative charge separation at 15 K (Fig. 5). The relatively small fraction of electrons on each flash which pass through F_X accounts for the inconsistency between the earlier EPR study, which showed near-quantitative photoreduction of F_A/F_B in $C565S_{PsaB}$ at 15 K in continuous light (Warren et al., 1993b), and the present work, which shows a low steady-state concentration of photoreduced F_X on continuous illumination at 9 K.

Comparison of the DM-PS I complex from the mutants with a wild-type PS I core, which is physically devoid of PsaC, shows an important difference between these preparations (Table 1). The ratio of the amplitude of the A_1^- components to that of F_X^- is considerably higher in the mutants (>4:1) than in the wild-type PS I core (<1:2) and can be explained assuming suppression of electron transfer from A_1^- to F_X. A similar consistency holds for the A_1^- and F_X^- components' amplitudes in the case of wild-type and $C565S_{PsaB}$ PS I preparations when F_A and F_B are prereduced with dithionite (Table 2). One possible explanation of these observations can be a decrease of the midpoint potential of the modified F_X cluster to a more electronegative value. The absolute midpoint potential of A_1 is not known with certainty; however, a plausible kinetic scheme for forward electron transfer in PS I has been presented in which the redox potentials of A_1 and F_X are very close (Sétif et al., 1993). Should the substitution of a serine for a cysteine drive the midpoint potential of F_X more electronegative, the quantum yield of forward electron transfer to F_A and F_B would depend on the equilibrium constant between A_1 and F_X and on the rate constants of back electron transfer between these reduced acceptors and P_{700}^+. These would result in a lower quantum efficiency of photoreduction of F_A and F_B and would be a direct consequence of an F_X cluster, which is ligated by only three thiolates. Based on data in this investigation, we conclude that a functional F_X is required for photoreduction of the F_A/F_B clusters at both room and cryogenic temperatures.

This work was supported by grants from the National Science Foundation (MCB-9205756) to J.H.G. and the Department of Energy (DE-FG02–90-ER20021) and M.S.U.-R.E.F. to L.M.

REFERENCES

Anderson, S. L., and L. McIntosh. 1991 Partial conservation of the 5′ *ndh*E-*psa*C-*ndh*D 3′ gene arrangement of chloroplasts in the cyanobacterium *Synechocystis* sp. PCC 6803: implications for NDH-D function in cyanobacteria and chloroplasts. *Plant Mol. Biol.* 16:487–499.

Beardwood, P., and J. F. Gibson. 1985. $[Fe_2S_2(OAr)_4]^{2-}$: iron-sulphur dimers with terminal phenolate ligands. *J. Chem. Soc. Chem. Commun.* 198:102–104.

Beinert, H., and A. J. Thomson. 1983. Three-iron clusters in iron-sulfur proteins. *Arch. Biochem. Biophys.* 222:333–366.

Belford, R. L., and M. J. Nilges. 1979. EPR Symposium, 21st Rocky Mountain Conference, Denver, CO, August 1979.

Brettel, K., P. Sétif, and P. Mathis. 1986. Flash-induced absorption changes in photosystem I at low temperature: evidence that the electron acceptor A_1 is vitamin K1. *FEBS Lett.* 203:220–224.

Brettel, K. 1989. New assignment for the 250 μs kinetics of photosystem I: $P\text{-}700^+$ recombines with A_1^- (not F_X^-). *Biochim. Biophys. Acta.* 976: 246–249.

Brettel, K., and J. H. Golbeck. 1995. Spectral and kinetic characterization of electron acceptor A_1 in a Photosystem I core devoid of iron-sulfur centers F_X, F_B and F_A. *Photosynth. Res.* In press.

Chamorovsky, S. K., and R. Cammack. 1982. Effect of temperature on the photoreduction of centers A and B in photosystem I, and the kinetics of recombination. *Biochim. Biophys. Acta.* 679:146–155.

Chamorovsky, S. K., and R. Cammack. 1982. Direct determination of the midpoint potential of the acceptor X in chloroplast photosystem I by electrochemical reduction and ESR spectroscopy. *Photobiochem. Photobiophys.* 4:195–200.

Cheng, H., B. Xia, G. H. Reed, and J. L. Markley. 1994. Optical, EPR, and H-1 NMR spectroscopy of serine-ligated [2Fe-2S] ferredoxins produced by site-directed mutagenesis of cysteine residues in recombinant *Anabaena* 7120 vegetative ferredoxins. *Biochemistry.* 33:3155–3164.

Chitnis, V. P., and P. R. Chitnis. 1993. PsaL subunit is required for the formation of Photosystem-I trimers in the cyanobacterium *Synechocystis* sp. *PCC-6803. FEBS Lett.* 336:330–334.

Crowder, M. S., and A. Bearden. 1983. Primary photochemistry of photosystem I in chloroplasts. Dynamics of reversible charge separation in open reaction centers at 25 K. *Biochim. Biophys. Acta.* 722:23–35.

Evans, M. C. W., and P. Heathcote. 1980. Effects of glycerol on the redox properties of the electron acceptor complex in spinach photosystem I particles. *Biochim. Biophys. Acta.* 590:89–96.

Fujinaga, J., J. Gaillard, and J. Meyer. 1993. Mutated forms of a [2Fe-2S] Ferredoxin with serine ligands to the iron-sulfur cluster. *Biochem. Biophys. Res. Commun.* 194:104–111.

Gao, J.-L., R. J. Shopes, and C. A. Wraight. 1991. Heterogeneity of kinetics and electron transfer equilibria in the bacteriopheophytin and quinone acceptors of reaction centers from *Rhodopseudomonas viridis. Biochim. Biophys. Acta.* 1056:259–272.

Golbeck, J. H., and J. M. Cornelius. 1986. Photosystem I charge separation in the absence of centers A and B. I. Optical characterization of center A2′ and evidence for its association with a 64-kDa peptide. *Biochim. Biophys. Acta.* 849:16–24.

Golbeck, J. H. 1987. Structure, function and organization of the photosystem I reaction center complex. *Biochim. Biophys. Acta.* 895:167–204.

Golbeck, J. H., T. Mehari, K. Parrett, and I. Ikegami. 1988. Reconstitution of the photosystem I complex from the P_{700}- and F_X-containing reaction center core protein and the F_A/F_B polypeptide. *FEBS Lett.* 240:9–14.

Golbeck, J. H., K. G. Parrett, T. Mehari, K. L. Jones, and J. J. Brand. 1988. Isolation of the intact photosystem I reaction center core containing P_{700} and iron-sulfur center F_X. *FEBS Lett.* 228:268–272.

Golbeck, J. H., and D. A. Bryant. 1991. Photosystem I. *Curr. Top. Bioenerg.* 16:83–177.

Høj, P., and B. L. Møller. 1986. The 110-kDa reaction center protein of photosystem I, P700-chlorophyll a-protein 1, is an iron-sulfur protein. *J. Biol. Chem.* 261:14292–14300.

Holden, H. M., B. L. Jacobson, J. K. Hurley, G. Tollin, B. H. Oh, L. Skjeldal, Y. K. Chae, H. Cheng, B. Xia, and J. L. Markley. 1994. Structure-function studies of [2Fe-2S] ferredoxins. *J. Bioenerg. Biomembr.* 26:67–88.

Krauss, N., W. Hinrichs, I. Witt, P. Fromme, W. Pritzkow, Z. Dauter, C. Betzel, K. S. Wilson, H. T. Witt, and W. Sänger. 1993. Three-dimensional structure of system-I of photosynthesis at 6 Angstrom resolution. *Nature.* 361:326–331.

Lüneberg, J., P. Fromme, P. Jekow, and E. Schlodder. 1994. Spectroscopic characterization of PS I core complexes from thermophilic *Synechococcus* sp.: identical reoxidation kinetics of A_1^- before and after removal of the iron-sulfur-clusters F_A and F_B. *FEBS Lett.* 338:197–202.

Mo'nne-Loccoz, P., P. Heathcote, D. J. Maclachlan, M. C. Berry, I. H. Davis, and M. C. W. Evans. 1994. Path of electron transfer in photosystem 1: direct evidence of forward electron transfer from A_1 to Fe-S_X. *Biochemistry.* 33:10037–10042.

Newman, T., F. J. de Bruijn, P. Green, K. Keegstra, H. Kende, L. McIntosh, J. Ohlrogge, N. Raikhel, S. Somerville, M. Thomashow, E. Retzel, and C. Somerville. 1994. Genes galore: a summary of methods for accessing results from large-scale partial sequencing of anonymous *Arabidopsis* cDNA clones. *Plant Physiol.* 106:1241–1255.

Ohad, N., and J. Hirschberg. 1992. Mutations in the D1 subunit of photosystem II distinguish between quinone and hebicide binding sites. *Plant Cell.* 4:273–282.

Parrett, K. G., T. Mehari, P. G. Warren, and J. H. Golbeck. 1989. Purification and properties of the intact P-700 and F_X-containing photosystem I core protein. *Biochim. Biophys. Acta.* 973:324–332.

Rodday, S. M., S. S. Jun, and J. Biggins. 1993. Interaction of the F(A)F(B)-containing subunit with the photosystem-1 core heterodimer. *Photosynth. Res.* 36:1–9.

Salifoglou, A., A. Simopoulos, A. Kostokas, R. W. Dunham, M. G. Kanatzidis, and D. Coucouvanis. 1988. Dimeric complexes containing the $[Fe_2S_2]^{2+}$ cores coordinated by non-sulfur terminal ligands. *Inorg. Chem.* 27:3394–3406.

Sauer, K., P. Mathis, S. Acker, and J. A. Van Best. 1978. Electron acceptors associated with P-700 in Triton solubilized photosystem I particles from spinach chloroplasts. *Biochim. Biophys. Acta.* 503: 120–134.

Sétif, P., and K. Brettel. 1990. Photosystem I photochemistry under highly reducing conditions: study of the P700 triplet state formation from the secondary radical pair ($P700^+$-A_1^-). *Biochim. Biophys. Acta.* 1020: 232–238.

Sétif, P., and K. Brettel. 1993. Forward electron transfer from phylloquinone-A_1 to iron-sulfur centers in spinach Photosystem-I. *Biochemistry.* 32:7846–7854.

Sétif, P., P. Mathis, and T. Vänngaard. 1984. Photosystem I photochemistry at low temperature. Heterogeneity in pathways for electron transfer to the secondary acceptors and for recombination processes. *Biochim. Biophys. Acta.* 767:404–414.

Sétif, P., and H. Bottin. 1989. Identification of electron-transfer reactions involving the acceptor A1 of photosystem I at room temperature. *Biochemistry.* 28:2689–2697.

Sétif, P., H. Bottin, and P. Mathis. 1985. Absorption studies of primary reactions in photosystem I. Yield and rate of formation of the P-700 triplet state. *Biochim. Biophys. Acta.* 808:112–122.

Shuvalov, V. A., A. M. Nuijs, H. J. Van Gorkom, H. W. J. Smit, and L. N. M. Duysens. 1986. Picosecond absorbance changes upon selective excitation of the primary electron donor P-700 in photosystem I. *Biochim. Biophys. Acta.* 850:319–323.

Sigfridsson, K., Ö. Hansson, and P. Brzezinski. 1995. Electrogenic light reactions in photosystem I: resolution of electron-transfer rates between the iron-sulfur centers. *Proc. Natl. Acad. Sci. USA.* 92:3458–3462.

Smart, L. B., P. V. Warren, J. H. Golbeck, and L. McIntosh. 1993. Mutational analysis of the structure and biogenesis of the Photosystem-I reaction center in the cyanobacterium *Synechocystis* sp. *PCC 6803. Proc. Natl. Acad. Sci. USA.* 90:1132–1136.

Van der Est, A., C. Bock, J. H. Golbeck, K. Brettel, P. Sétif, and D. Stehlik. 1994. Electron transfer from the acceptor A_1 to the iron-sulfur centers in Photosystem I as studied by transient EPR spectroscopy. *Biochemistry.* 33:11789–11797.

Warren, P. V., J. H. Golbeck, and J. T. Warden. 1993a. Charge recombination between P_{700}^+ and A_1^- occurs directly to the ground state of P_{700} in a Photosystem I core devoid of F_X, F_B, and F_A. *Biochemistry.* 32:849–857.

Warren, P. V., L. B. Smart, L. Mcintosh, and J. H. Golbeck. 1993b. Site-directed conversion of cysteine-565 to serine in PsaB of Photosystem-I results in the assembly of [3Fe-4S] and [4Fe-4S] clusters in F_X: a mixed-ligand [4Fe-4S] cluster is capable of electron transfer to F_A and F_B. *Biochemistry.* 32:4411–4419.

Webber, A. N., P. B. Gibbs, J. B. Ward, and S. E. Bingham. 1993. Site-directed mutagenesis of the Photosystem I reaction center in chloroplasts. *J. Biol. Chem.* 268:12990–12995.

Williams, J. G. K. 1988. Construction of specific mutations in photosystem II photosynthetic reaction center by genetic engineering methods in *Synechocystis* 6803. *Methods Enzymol.* 167:766–778.

Yu, J., Smart, L. B., Jung, Y-S., Golbeck, J. H., and McIntosh, L. 1995. Absence of the PsaC subunit allows assembly of the photosystem I core but prevents the binding of PsaD and PsaE in *Synechocystis* sp. PCC 6803. *Plant Mol. Biol.* In press.